Article ID: 1003- 6326(2004)05-0840-06

Crystallization kinetics and induced magnetic properties of bulk (Fe, Co)-Zr-Nd-B metallic glass①

LI Fu-shan(李福山)[1], ZHANG Tao(张 涛)[2], GUAN Shao-kang(关绍康)[1], SHEN Ning-fu(沈宁福)[1]
(1. Research Center for Materials, Zhengzhou University, Zhengzhou 450002, China;
2. School of Materials Science and Engineering,
Beijing University of Aeronautics and Astronautics, Beijing 100083, China)

Abstract: Crystallization kinetics and phase transformation of bulk $Fe_{64}Co_7Zr_6Nd_3B_{20}$ metallic glass were studied by X-ray diffractometry (XRD), differential scanning calorimetry (DSC) and transmission electron microscopy (TEM). Based on the Kissinger analyses, the activation energies for the nucleation and growth during the first, second and third crystallization stages of the metallic glass are determined to be 294, 475 and 365 kJ/mol, respectively, and the activation energy for the glass transition is determined to be 1 242 kJ/mol. The Johnson-Mehl-Avrami (JMA) analysis under the isothermal condition reveals that the crystallization process is a three-dimensional controlled growth of nuclei at a constant nucleation rate. The crystalline grains are in the size of less than 50 nm after the selected annealing treatments. In the completely crystallized state, the alloy exhibits the maximum coercivity (H_c) of 34.8 kA/m and corresponding energy product of 11 kJ/m^3.

Key words: nanocrystallization; kinetics; bulk Fe-based metallic glass; magnetic properties
CLC number: TG 141 **Document code:** A

1 INTRODUCTION

Since the first synthesis of an amorphous alloys in an Au-Si system by melt-spun technique in 1960[1], a great number of amorphous alloys have been synthesized in the last four decades. Metallic glasses are considered as a more and more attractive area owing to their promising mechanical and/or functional properties. Among these alloys, Fe-based metallic glasses have been particularly investigated due to their excellent corrosion resistance and good soft magnetic properties (high saturation magnetization, low coercivity and maximum permeability). Some Fe-based amorphous alloy systems with ferromagnetism at room temperature have been found. Bulk Fe-based metallic glasses[2-4], such as Fe-(Al, Ga)-(P, C, B, Si)[5, 6], Fe-(Mo, Co, Ga)-(P, C, B, Si)[7, 8], Fe-(Co, Ni)-M-B (M= Zr, Hf, Nb, Ta, Mo, W)[9, 10] and Fe-Ni-P-B[11, 12] were synthesized in the recent years. Fe-based metallic glasses containing rare earth elements (RE) have appeared to be a new type of ferromagnetic amorphous materials with unique magnetic properties. The current type of bulk ferromagnetic metallic glasses of Fe-Co-Ln-B[13, 14] with a wide supercooled liquid region before crystallization and soft magnetic properties have been prepared. However, there has not been reported on synthesizing this type of bulk metallic glass with the coexistence of early transition metal like Zr. The authors have investigated the glass-forming ability, thermal stability and magnetic properties of Fe-Co-Zr-Nd-B[15] alloys, and successfully produced bulk $Fe_{64}Co_7Zr_6Nd_3B_{20}$ metallic glasses with a diameter of 1mm by the method of copper mould casting. In the present paper, the kinetics of crystallization, the phase transformation and the changes of magnetic properties are reported.

2 EXPERIMENTAL

The master alloy ingots were prepared in the nominal composition of $Fe_{64}Co_7Zr_6Nd_3B_{20}$ (all alloy compositions are given in nominal atomic percents) by arc melting the mixtures of Fe(mass fraction) 99.9% with low C, Co 99.9%, Zr 99.9%, Nd 99.9% and B 99.5% under argon atmosphere. The bulk glassy samples in the shape of rod with a diameter of 1mm and length of 3-5 cm were produced by copper mould injection casting under argon atmosphere. The structures of the samples were examined by XRD and TEM. Thermal stability was measured by DSC under argon atmosphere at heating rate of 0.67 K/s. The saturation magnetization was measured with VSM under a maximum applied magnetic field of 800 kA/

① **Foundation item:** Project(0311050200) supported by the Natural Science Foundation of Henan Province, China; project(2003430209) supported by the Natural Science Foundation of the Education Bureau of Henan Province, China
Received date: 2004-03-17; **Accepted date:** 2004-06-06
Correspondence: LI Fu-shan, Tel: +86-371-3887502; Fax: +86-371-3887508; E-mail: fsli@zzu.edu.cn;

m at room temperature. The coercive force was measured with a *J-H* loop tracer. The samples for TEM were prepared by the ion thinning technique. Phase transformations in as-solidified rod samples were studied by DSC at different heating rates ranging from 0.17 to 1.33 K/s and isothermal calorimetry. During isothermal scanning the samples were heated to the testing temperatures at heating rate of 1.67 K/s. The isothermal annealing of the samples encapsulated in quartz tubes was carried out in a vacuum of 3×10^{-3} Pa. The annealing temperature was maintained with a precision of ± 1 K.

3 RESULTS AND ANALYSIS

3.1 Crystallization process and structures

Fig. 1 shows the DSC pattern of the as-solidified sample taken at a heating rate of 0.67 K/s. The distinct exothermic peaks caused by crystallization at three well-separated steps can be observed for the selected bulk metallic glass. The bulk metallic glasses exhibit T_g at 844 K and T_x at 911 K, where T_g and T_x are glass transition temperature and crystallization temperature, respectively, thus resulting the values of T_x reaching 67 K. The as-solidified samples were then studied by DSC with different heating rates and annealed at different temperatures corresponding to the exothermal heat effects observed. Fig. 2 shows the XRD patterns of the samples in as-solidified and other different isothermal annealing states. Fig. 2(a) shows a broad halo peak in the vicinity of $2\theta = 44°$, which indicates the formation of a single Fe-based glassy phase in as-solidified ribbon samples. Fig. 2 (b), (c), (d) and (e) show the XRD patterns of the metallic glasses after isothermal annealing at 877 K for 1 200 s, 925 K for 360 s, 1 000 K for 360 s and 1 150 K for 360 s, respectively . Fig. 2(b) reveals only a weak crystalline transformation at the mid T_g occurring unappreciably in amorphous matrix even if the annealing time is much longer than that of the samples annealed at the temperatures of the ends of

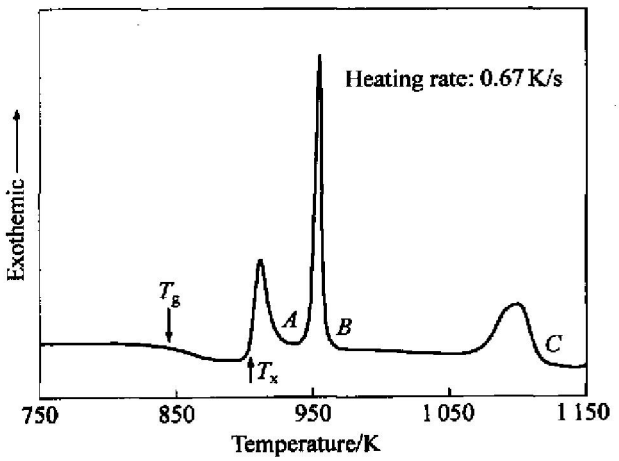

Fig. 1 DSC pattern of bulk $Fe_{64}Co_7Zr_6Nd_3B_{20}$ glassy alloy

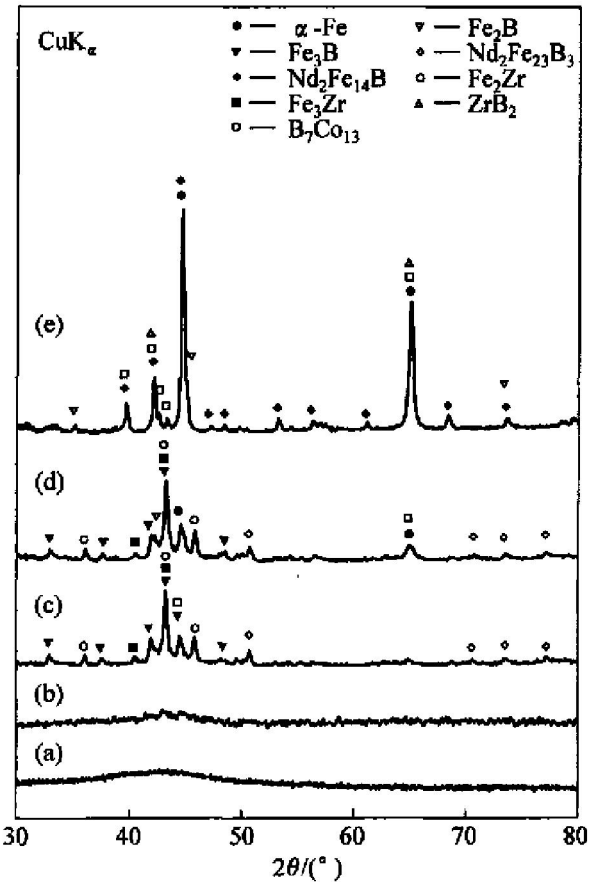

Fig. 2 XRD patterns of bulk $Fe_{64}Co_7Zr_6Nd_3B_{20}$ alloy with different isothermal anaealing states
(a) —As-solidified;
(b) —Annealing at 877 K for 1 200 s;
(c) —Annealing at 925 K for 360 s;
(d) —Annealing at 1 000 K for 360 s;
(e) —Annealing at 1 150 K for 360 s

the first, second, and final exothermic effects, of which crystallization can be observed obviously. The crystallization from the supercooled liquid of the glassy alloys occurred through three stages as follows: $Am \rightarrow Am' + Nd_2Fe_{23}B_3 + Fe_3B + Fe_3Zr + B_7Co_{13} \rightarrow Am'' + \alpha\text{-}Fe + Nd_2Fe_{23}B_3 + Fe_3B + Fe_3Zr + B_7Co_{13} \rightarrow \alpha\text{-}Fe + Nd_2Fe_{14}B + Fe_2B + Fe_2Zr + ZrB_2$, which correspond to the fully crystalline structures after isothermal annealing identified in Fig. 2(c), (d) and (e), respectively. Fig. 3 shows the microstructure of the bulk Fe_{64}-$Co_7Zr_6Nd_3B_{20}$ metallic glasses after isothermal annealing at 1 150 K for 360 s. The average grain size is less than 50 nm for all the α-Fe, $Nd_2Fe_{14}B$, Fe_2B, Fe_2Zr and ZrB_2 phases. The insert part in Fig. 3(a) is a selected area electron diffraction (SAED).

3.2 Kinetic studies of crystallization

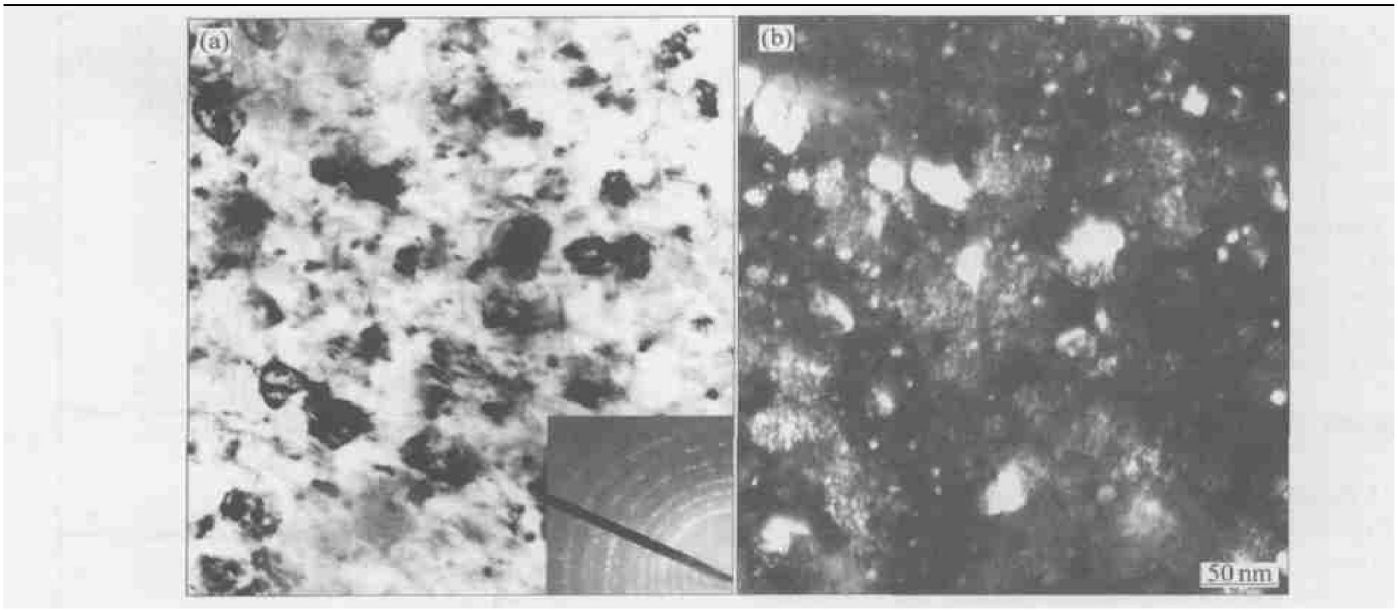

Fig. 3 Microstructures of bulk $Fe_{64}Co_7Zr_6Nd_3B_{20}$ glassy alloy completely annealing at 1 150 K for 360 s
(a) —TEM bright-field image and SAED; (b) —Dark-field image

3.2.1 Kissinger analyses of DSC patterns

DSC patterns taken at different heating rates were used for Kissinger analysis to determine the activation energy (E_{act}) of the nucleation and the growth of the primary phase[16-18] in the bulk metallic glass. The method is based on the fact that the observed temperature of a peak depends on the scan rate, $S = dT/dt$, *of the experiment and the assumption that crystallized fraction* (x_c) *of the amorphous phase transformed at the peak temperature is independent of* S. *The peak temperatures,* T_p, *shift towards high values with increasing scanning rates. Such shifts of peak temperatures corresponding to definite fraction* (x_c) *of the* $Fe_{64}Co_7Zr_6Nd_3B_{20}$ *amorphous phase transformed can be seen in Fig. 4(a). The* E_{act} *and* x_c *are related by*

$$dx_c/dt = k_0(1-x_c)\exp(-E_{act}/RT) \quad (1)$$

where k_0 *is pre-exponetial factor in the Arrhenious equation. Based on the fact that the derivative* dx/dt *attains a maximum value at* T_p, *the Kissinger expression relates* T_p *to* S

$$\ln(S/T_p^2) = -E_{act}(RT_p) + \ln(Rk_0E_{act}) \quad (2)$$

The plots of $[\ln(S/T_p^2)]$ versus $(1/T_p)$ are shown in Fig. 4(b). The linear regressions of Eqn. (2) for T_p1, T_p2 and T_p3 of the first, second and third extherms are well fit for linearity. Although the method was originally derived to analyze the peak temperature, it can also be applied to T_g, which is validated by the high linearity of the regression fit of Eqn. (2). The reason perhaps is that T_g is defined to be the temperature at which the transform ation from glassy to supercooled liquid state is half complete. The activation energies, E_{actp1}, E_{actp2}, E_{actp3} and E_{actg} for T_{p1}, T_{p2}, T_{p3} and T_g can be obtained easily from the slopes of the regressive plots, which are

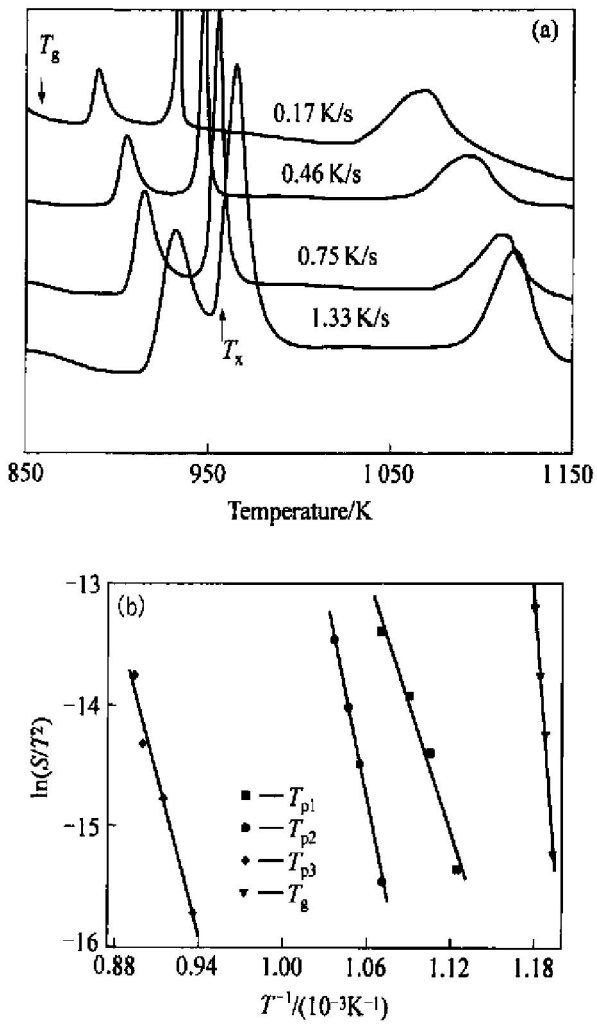

Fig. 4 Constant heating rate DSC scan results for bulk $Fe_{64}Co_7Zr_6Nd_3B_{20}$ glassy alloy
(a) —DSC patterns taken at four different heating rates;
(b) —Kissinger plots for glass transition and three exotherm peaks

294, 475, 365 and 1 242 kJ/mol, respectively. The completion of the transition from the glass to the supercooled liquid state needs much larger activation energy than that of the succedent crystallization.

3.2.2 Kinetic analyses of crystallization

Fig. 5(a) shows the heat flow $h(t, T)$ measured by isothermal DSC scans for the bulk $Fe_{64}Co_7Zr_6Nd_3B_{20}$ glass at different annealing temperatures (T_a) in the supercooled liquid region prior to the crystallization. The initiative times for the crystallization were reduced to the same by excluding the relative incubation times for the convenience of kinetic parameter calculation. Assuming that the integrated enthalpy is proportional to the crystallized fraction, $x_c(t, T)$, the $x_c(t, T)$ after a time t at the constant temperature (T) can be expressed as

$$x_c(t, T) = \frac{\int_0^t h(t, T)\,dt}{\int_0^\infty h(t, T)\,dt} \quad (3)$$

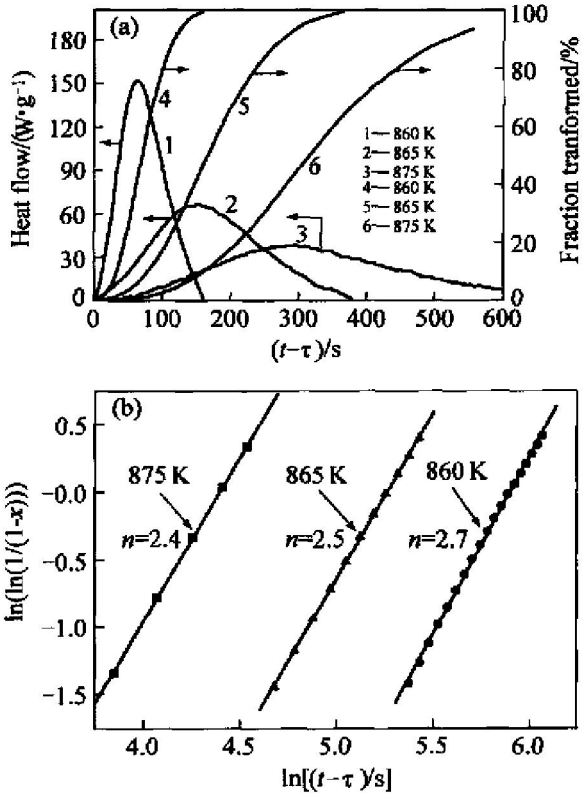

Fig. 5 Isothermal DSC data of bulk $Fe_{64}Co_7Zr_6Nd_3B_{20}$ glassy alloy

(a) —Isothermal calorimetry taken at three different temperatures (incubation period is excluded) and fractions transformed;

(b) —Avrami plots for $0.1 \leqslant x_c \leqslant 0.9$

The $x_c(t, T)$ plot (the dashed lines) takes the shape of the customary sigmoidal shape.

Then the crystallization kinetics was studied in terms of the theory of JMA analysis[19, 20]. The JMA equation is written as

$$x_c(t, T) = 1 - \exp(-b(t-\tau)^n) \quad (4)$$

where b is a constant, τ is the incubation time, and n is the Avrami exponent. By logarithm conversion, Eqn. (4) can be also written as

$$\ln(-\ln(1-x_c)) = \ln b + n\ln(t-\tau) \quad (5)$$

Fig. 5(b) shows the plot of Eqn. (5) for the present bulk metallic glass, which is a linear regression with a correlation coefficient better than 0.996 for $0.1 \leqslant x_c \leqslant 0.9$. The slopes of the regressive fits (n) are 2.7, 2.5 and 2.4 at 860, 865 and 875 K, respectively, with an average value of 2.5, which corresponds to the three-dimensional diffusion-controlled growth of nuclei at a constant nucleation rate[18, 21].

The incubation time and crystallizing transition time fit in with Arrhenious behavior, which are

$$\tau = \tau_0 \exp(E_\tau / RT) \quad (6)$$

$$t - \tau = t_0 \exp(E_x / RT) \quad (7)$$

where E_τ and E_x are the apparent energy for reaching steady state nucleation rate and the activation energy, respectively. For the overall crystallization process, τ_0 and t_0 are constants. By the Arrhenius analysis, the value of E_x for $x_c = 0$ was determined to be 373 kJ/mol, and the values of E_x for different x_c are basically the same with an average of (597 ±20) kJ/mol. For the present bulk metallic glasses, the incubation times at 910, 850, 800 and 650 K were inferred to be 47 s, 25.5 min, 11.5 h and 548 a, respectively, from the extrapolation of Eqn. 6. The crystallizing transition times at different temperatures can also be derived from the extrapolation of Eqn. 7, e.g. the crystallizing transition times of $x_c = 0.20$ at 910, 850, 800 and 700 K are 1.4 s, 9 min, 40 h and 391 A, respectively. When the temperature is high than T_g as at 844 K(see Fig. 1), the extrapolated incubation and crystallizing transition times are very short and decrease rapidly with the small increase of annealing temperature, for instance, the extrapolated incubation time decreases from 25.5 min at 850 K to 47 s at 910 K just above T_x. On the contrary, when it is below T_g, the extrapolated incubation and crystallizing transition times are very long and increase rapidly with the small decrease in annealing temperatures, e.g. the extrapolated incubation time increases from 25.5 min at 850 K to 11.5 h at 800 K just below T_g. If annealed below 650 K, the studied metallic glasses can only begin to crystallize after 548 a. The changes in crystallizing transition times at different temperatures show the same tendency as that of the extrapolated incubation time. Fig. 2(b) shows the XRD result for the bulk $Fe_{64}Co_7Zr_6Nd_3B_{20}$ glasses after annealed at 877 K for 1 200 s. Compared to Fig. 2(c) which shows the XRD result for the glasses after annealed at 925 K for 360 s, it can be clearly observed that an increase of only 48 K greatly enhanced the crystallizing rate. Consequently, the analyses of the DSC kinetic data and experimental XRD results indicate that the amorphous phase should be

stable at least the temperature up to 650 K (perhaps even higher).

3.3 Nanocrystallization-induced transformation of magnetic properties

The crystallization of the present Fe-based glass containing RE element induces the transformation from soft magnetic properties to hard ones. Fig. 6 shows the hysteresis *J-H* loops of the bulk $Fe_{64}Co_7Zr_6Nd_3B_{20}$ metallic glass annealed at different T_a for the same annealing time. In order to compare the changes in magnetic properties, Fig. 6 also includes the insert part of the hysteresis *J-H* loop of the studied metallic glass in the as-quenched amorphous state, which exhibits good soft magnetic properties of saturation magnetization (J_s) at 1.26 T and H_c at 4.2 A/m. The values of H_c increase greatly with T_a from 4.2 A/m in the amorphous state to 14.0, 22.1 and 34.8 kA/m in the nanocrystalline state after annealed at 925, 1 000 and 1 150 K, respectively, all for 6 min. The energy product also increases saliently with the annealing temperature, which are 3, 5 and 11 kJ/mol for the crystalline state after annealed at 925, 1 000 and 1 150 K, respectively. The crystallization during annealing results in the emergence of hard magnetic phases of the $Nd_2Fe_23B_3$ (when T_a= 1 000 K) and $Nd_2Fe_{14}B$ (when T_a= 1 150 K). The maximum energy product reached 11 kJ/mol at the complete crystalline state. Thus, it can be concluded that the energy product increases with the emergence and increase of the resultant α-Fe and $Nd_2Fe_{14}B$ hard magnetic phases, compared to the decrease and dissolution of Fe_3Zr, B_7Co_13 and $Nd_2Fe_23B_3$ hard magnetic phases. The transformation from soft magnetic properties to hard ones for the Fe-based glasses is due to the exchange magnetic coupling interaction between α-Fe and the hard magnetic phases[22].

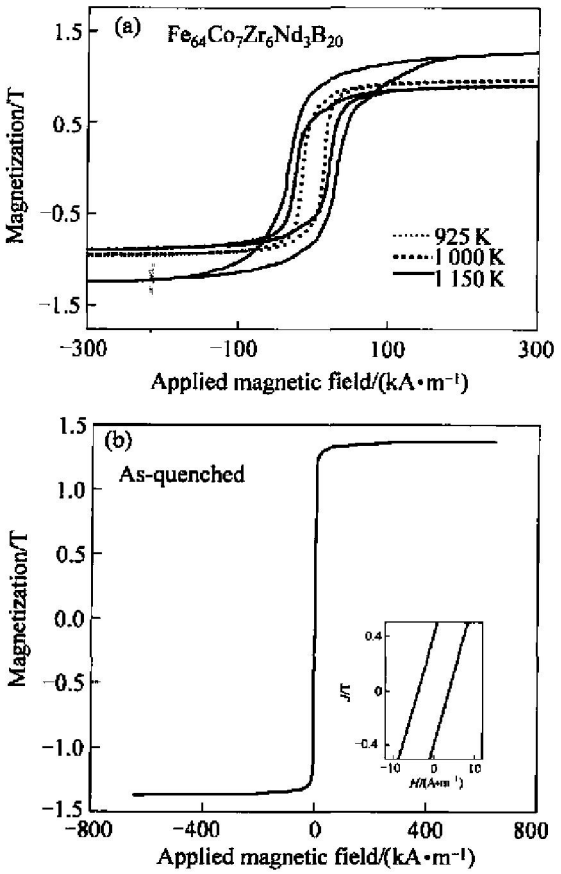

Fig. 6 Hysteresis *J-H* loops of $Fe_{64}Co_7Zr_6Nd_3B_{20}$ alloy annealed at different T_a for 360 s (a) and hysteresis *J-H* loop of $Fe_{64}Co_7Zr_6Nd_3B_{20}$ glassy alloy in as-quenched amorphous state (b)

4 CONCLUSIONS

1) The fundamental assumption of the Kissinger derivation is satisfactory not only for the crystallization peak temperatures but also for the glass transition temperature of the bulk Fe_{64}-$Co_7Zr_6Nd_3B_{20}$ metallic glass with a large supercooled liquid region. The DSC kinetic measurements indicate that the glassy alloy should be practically stable at least the temperature up to 650 K.

2) The crystalline grains are in the size less than 50 nm for the selected annealing technique. The nanocrystallization induces the transformation from soft magnetic properties to hard ones for this bulk metallic glasses. The maximum energy product reaches 11 kJ/mol for the present bulk Fe-based glass after annealed at 1150 K for 6 min.

ACKNOWLEDGEMENTS

The authors are indebted to the related researcher of Advanced materials Laboratory and Inoue Laboratory in Institute for Materials Research, the Tohoku University. The work was supported by them.

REFERENCES

[1] Klement W, Willens R H, Duwez P. Noncrystalline structure in solidified gold-silicon alloys [J]. Nature, 1960, 187: 867-868.

[2] Inoue A. Stabilization of metallic supercooled liquid and bulk amorphous alloys[J]. Acta Mater, 2000, 48: 279-306.

[3] Inoue A, Takeuchi A. Recent progress in bulk glassy alloys[J]. Mater Trans, 2000, 43: 1892- 1906.

[4] Makino A, Inoue A, Mizushima T. Soft magnetic properties of Fe-based bulk amorphous alloys [J]. Mater Trans JIM, 2000, 41: 1471-1477.

[5] Inoue A, Murakami A, Zhang T, et al. Thermal stability and magnetic properties of bulk amorphous Fe-Al-Ga-P-C-B-Si alloys[J]. Mater Trans JIM, 1997, 38: 189-196.

[6] Inoue A, Gook J S. Effect of additional elements (M) on the thermal stability of supercooled liquid in $Fe_{72-x}Al_5Ga_2P$ 11 $C_6B_4M_x$ glassy alloys [J]. Mater Trans JIM, 1996, 37: 32-38.

[7] Shen B L, Koshiba H, Kimura H, et al. Bulk glassy Fe-Co-Ga-P-C-B alloys with high glass-forming ability, high saturation magnetization and good soft magnetic properties[J]. Mater Trans JIM, 2002, 41: 1675 - 1678.

[8] Shen B L, Koshiba H, Kimura H, et al. High strength and good soft magnetic properties of bulk glassy Fe-Mo-Ga-P-C-B alloys with high glass-forming ability [J]. Mater Trans JIM, 2000, 41: 1478 - 1481.

[9] Chiriac H, Lupu N. Bulk amorphous (Fe, Co, Ni)$_{70}$(Zr, Nb, M)$_{10}$B$_{20}$(M = Ti, Ta or Mo) soft magnetic alloys [J]. J Magn Magn Mater, 2000, 215 - 216: 394 - 396.

[10] Koshiba H, Inoue A, Makino A. Nanocrystallization and magnetic properties of $Fe_{56}Co_7Ni_7Zr_2M_8B_{20}$ (M = Nb or Ta) glassy alloys[J]. Nano Mater, 1997, 8: 997 - 1005.

[11] Li F S. Study on Fe-based glassy alloys with soft magnetic properties[J]. J Zhengzhou University (Engineering Science), 2002, 23: 30 - 32. (in Chinese)

[12] Shen T D, Shwarz R B. Bulk ferromagnetic glasses in the Fe-Ni-P-B System[J]. Acta Mater, 2001, 49: 837 - 847.

[13] Zhang W, Inoue A. Formation and soft magnetic properties of (Fe, Co)-RE-B glassy alloy with large thickness[J]. Mater Trans, 2001, 42: 1835 - 1838.

[14] Zhang W, Long Y, Imafuku M, et al. Thermal stability and soft Magnetic properties of (Fe, Co)-(Nd, Dy)-B glassy alloys with high boron concentrations [J]. Mater Trans, 2002, 43: 1974 - 1978.

[15] Li F S, Zhang T, Guan S K, et al. Thermal stability and soft Magnetic properties of (Fe, Co)-Zr-Nd-B amorphous alloys[J]. J Rare Earths, 2003, 21(Suppl): 190 - 193.

[16] Kissinger H E. Reaction kinetics in differential thermal analysis[J]. Anal Chem, 1957, 29: 1702 - 1706.

[17] Smith G W, Pinkerton F E, Moleski J J. Determination of phase stability in a bulk amorphous alloy by differential scanning calorimetry[J]. Thermochimica Acta, 1999, 342: 31 - 39.

[18] Louzguine D V, Inoue A. Nanocrystallization of Cu-(Zr or Hf)-Ti metallic glasses[J]. J Mater Res, 2002, 17: 2112 - 2120.

[19] Jonhson W A, Mehl R F. Reaction kinetics in processes of nucleation and growth[J]. Trans Amer Inst Min Eng, 1939, 135: 416 - 442.

[20] Avrami M. Kinetics of phase change III —Granulation phase change and microstructure[J]. J Chem Phys, 1941, 9: 177 - 184.

[21] Christian J W. The Theory of Transformations in Metals[M]. Oxford, UK: Pergamon Press, 1975. 542.

[22] Inoue A, Fujita K, Zhang T, et al. Synthesis of glassy Fe-Co-Nd-Zr-B alloys and their crystallization-induced magnetic properties[J]. Mater Trans, JIM, 1998, 39: 327 - 333.

(Edited by LONG Huai-zhong)